TMS2013 Annual Meeting Supplemental Proceedings
TMS (The Minerals, Metals & Materials Society), 2013

HYDROGEN-DISLOCATION INTERACTIONS AND CROSS-SLIP INHIBITION IN FCC NICKEL

Yizhe Tang[1], Satish I. Rao[2], Jaafar A. El-Awady[1]

[1]Johns Hopkins University; 3400 North Charles Street; Baltimore, MD, 21218, USA
[2]UES, Inc.; 4401 Dayton-Xenia Rd.; Dayton, OH, 45432-1894, USA

Keywords: Hydrogen, Dislocations, Embrittlement, Cross-slip

Abstract

In this study, H-dislocation interactions are investigated using Molecular Statics simulations. The binding energies of H to both edge and screw dislocations are computed and it is shown that Shockley partial cores have the strongest interactions with H. The stacking fault (SF) width can either increase or decrease depending on the H-occupying sites relative to the strongest binding sites. The unstable SF energy is shown to decrease with increasing H-content, indicating increased lattice resistance to shear; whereas the stable SF energy decreases due to the negative binging energy of H to the dislocation. In the case of dislocation-forest intersection induced cross-slip [Satish Rao *et al* 2009-2012], hydrogen in the stacking fault pins partial dislocations and increases the cross-slip activation energy. As a result, the instantaneous cross-slip reaction could be fully inhibited by a sufficient high H-content.

Introduction

Pernicious effects of hydrogen (H) on the mechanical properties of metals have been documented in many materials [1,2,3], and various experimental studies [4-12] have been carried out to explore the nature of H-degradation in metals. Although such experimental investigations provide insights on the effects of H on the macroscopic properties of metals, they are highly dependent on the experimental setup and unintentional damage that may be introduced in the tested material. Thus, the results obtained are sometimes conflicting and contradictory [4]. For example, for iron, aluminum and nickel, both a decrease [5,6] and an increase [7,8] in flow stress have been reported. Similarly, H has been linked to the degradation of fatigue properties and fatigue crack growth in steels [9], which is contrary to more recent results suggesting that H can enhance fatigue properties [10,11]. In addition, hydrogen embrittlement (HE) processes occur at the atomic scale (e.g. dislocation core, crack tip etc.) where exact mechanisms are not easily identified experimentally. Thus, HE remains one of the most severe and controversial types of failure.

Atomistic simulations can provide details of deformation and fracture at the atomic level, enabling better understanding of relevant microscopic mechanisms. Early molecular dynamics (MD) study of H-effects on metals was performed by Daw *et al.* in 1986 [12] followed by various studies mostly focusing on dislocation emission and plasticity around crack-tips [13,14]. One the other hand, pre-existing dislocations are ubiquitous and one of the most important defects controlling plasticity in metals. However, atomistic simulations addressing H interaction with pre-existing dislocations received less attention. Wen *et al.* [15,16], using molecular statics (MS) and the embedded-atom method (EAM), showed that the stacking fault (SF) width of a screw dislocation in nickel (Ni) increases with increasing H-concentration (uniformly distributed on the dislocation glide plane). They hypothesized that the increase in SF width is due to the

decrease in stacking fault energy (SFE) in the presence of H. On the contrary, more recent EAM-based Monte Carlo simulations concluded that the SF width decreases significantly, and that the stable SFE increases with increasing H-concentration [17]. Thus far, the reported atomic mechanisms of H-dislocation interactions remain contradictory and incomplete.

To address some of these issues, H interactions with pre-existing screw and edge dislocations in a Ni-H single crystal system are carefully evaluated in the present study. First, the binding energies of an interstitial H atom to both edge and screw dislocations are calculated. In view of these results, the repulsive and attractive H-dislocation interactions, as well as the SF width then are computed as a function of the H-occupying sites. The generalized stacking fault energy (GSFE) is also calculated as a function of H-concentration. Finally, the instantaneous cross-slip induced by dislocation-intersection is studied in the presence of H in the SF.

Computational Method

Molecular statics simulations were performed using LAMMPS code [18].The EAM potential used in this study is that for FCC Ni-H systems developed by Angelo *et al* [19,20]. The conjugate gradient (CG) method, and an energy tolerance of 10^{-12} were employed during energy minimization. The common neighbor analysis (CNA) technique [21] was used to identify defects (i.e. non-FCC atoms), while visualization of the atomic configurations were obtained using the Visual Molecular Dynamics (VMD) [22].

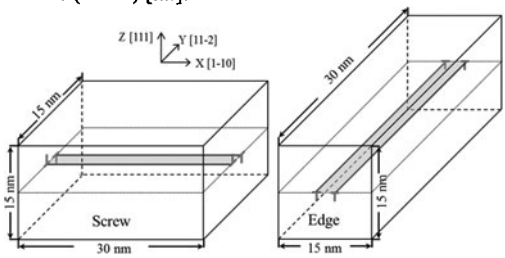

Figure 1. Schematic showing dissociated screw and edge dislocations. The Shockley partials are denoted by 'T' or inverse 'T' symbols and the shaded areas represent stacking fault.

A schematic of the simulation cells are shown in Figure 1. The X, Y and Z axes were oriented along the $[1\bar{1}0]$, $[11\bar{2}]$ and $[111]$ directions, respectively. The total number of atoms in all simulation cells was ~700,000. The modeled edge and screw dislocations had Burgers vector $b = a_0/2\,[1\bar{1}0]$ on the (111) plane, and were introduced at the center of the simulation cells using their anisotropic elastic displacement fields [23]. Here, $a_0 = 0.352\,\text{nm}$ is the lattice constant for FCC Ni. For screw dislocation, periodic boundary conditions (PBCs) were employed along the X-direction (i.e. dislocation line direction) to mimic an infinite-long dislocation, while free boundary conditions were employed along the Z-direction. In addition, PBCs were also introduced in the Y-direction (i.e. dislocation glide direction), to avoid dislocation-surface interaction [24]. For edge dislocation, PBCs were employed along both X- and Y-directions, while free boundary conditions were employed in the Z-direction. As seen in Figure 1, the upper and lower halves of the sample undergo tensile and compressive strain, respectively.

After introducing an edge or a screw dislocation into the simulation cell, energy minimization was performed, and both edge and screw dislocations dissociated into a stacking fault (SF) bound by two $a_0/6<112>$ Shockley partials. The SF width was with 2.74 nm and

1.51 nm for edge and screw dislocation, respectively. A single H atom was then introduced at various positions in the vicinity of the edge and screw dislocations to compute the binding energy. Preferential H-occupation sites were determined from the binding energy curves [24], to be: octahedral-sites (O-sites) in the perfect FCC crystal region, tetrahedral-sites (T'-sites) in the SF, and both O'- and T'-sites in the glide plane near the partial cores. The naming convention here is according to the H relative positions to the reference lattice, chosen along the lower half (Z-direction) of the lattice. The O'-site and T'-site correspond to the O-site and T-site in a defective lattice (i.e. in the SF and dislocation core).

Simulations to identify the effects of H on SF width were performed by introducing arrays of H-atoms parallel to the dislocation line (line density of 2.00 atoms/nm) at various occupying sites in the vicinity of the dislocation. Energy minimization was then performed and all atoms were allowed to relax. Generalized stacking fault energy (GSFE) [25] calculations of the primary slip system $(111)/[11\bar{2}]$ with and without H were evaluated by shearing the upper half relative to the lower half of the simulation volume in the Y-direction by the fault vector f in unit of $a_0/6[11\bar{2}]$. For further details about the simulations, the reader is referred to Ref. [24]. For the cross-slip simulations, the same dislocation configuration as used by Rao *et al.* [26] was adopted. The forest dislocation was introduced after the screw was fully relaxed, and then H arrays were introduced to T'-sites in the SF of the screw dislocation.

Results and Discussion

Binding Energy of Hydrogen to Edge and Screw Dislocations

The binding energies, E_b, of H to edge and screw dislocations as a function of distance between H and dislocation centerline are shown in Figure 2 (see details in Ref. [24]).

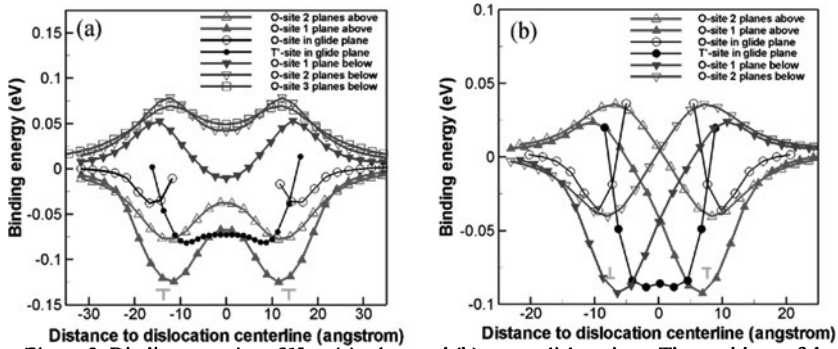

Figure 2. Binding energies of H to (a) edge; and (b) screw dislocations. The positions of the Shockley partial cores are shown by 'T' and inverse 'T' symbols.

As shown in Figure 2a, the binding energy curves of H to an edge dislocation are symmetric with respect to the dislocation centerline (X=0). This is attributed to the symmetry of the stress field of the edge dislocation. Here, the dislocation centerline is defined as the midline between the two Shockley partials. For H at O-sites on one plane above the glide plane were the dislocation produces a tension stress-field, a negative binding energy is observed with a global minimum when H is at a horizontal distance $|X|$=12 angstrom from the dislocation centerline. Thus, an attractive or a repulsive force will develop if H occupies a site other than the minimum

binding energy site [24]. When H occupies O-sites on two planes below the glide plane were the dislocation produces a compression stress-field a positive binding energy is observed, and two global maxima are observed when H is at a distance |X|=13 angstrom from the dislocation centerline. An attractive or a repulsive force will also develop if H occupies a site other than the minimum site [24]. If H is introduced to three or more planes below the glide plane, or further from the dislocation centerline (|X|>13), the binding energy approaches to zero and the H-dislocation force weakens.

For H on the glide plane, the binding energy of H at O-sites decreases as H approaches the partial core, and two minima are observed when H is at |X| = 15 angstrom. When H occupies an O-site closer to the partial core, the binding energy rises again. On the other hand, for H occupying T'-site in the SF, the binding energy decreases as H occupies sites away from the edge dislocation centerline and closer to the partial cores, and two minima are observed when H is at |X| = 9 angstrom. As the H-atom occupies sites even closer to the partial cores the binding energy increases. A repulsive or attractive forces will develop between H-arrays on the glide plane at O- and T'-sites and the edge dislocation, depending on their relative positions [24].

As shown in Figure 2b, the binding energy curves of H to screw dislocation are anti-symmetric with respect to Y = 0, due to the anti-symmetry in the screw stress field. For H at O-sites in planes above the glide plane, a negative binding energy is obtained near one partial core (tension region); while at the other core (compression region) a positive binding energy is obtained. For H on planes below the glide plane, the behavior is reversed. On the glide plane, the minima in the SF are not as obvious as that for the edge case, due to the relatively narrower SF width of the screw dislocation. H at T'-site in the SF has almost constant binding energies when $|Y| \leq 4.5$ angstrom, then the energy rapidly increases when $|Y| > 4.5$ angstrom.

Hydrogen Effects on the Stacking Fault Width

Wen *et al.* performed MD simulations on a Ni-H system, and showed that H uniformly distributed on the glide plane will increase the width of a screw dislocation [15,16]. On the contrary to those results, more recent EAM-based Monte Carlo simulations of Ni-H concluded that the SF width of an edge dislocation decreases significantly with increasing H-concentration [17]. To address these conflicting results, we re-evaluate the effect of H on the SF width in view of the accurate H preferential occupying-sites in the perfect FCC lattice, dislocation SF, and the cores of the dissociated dislocation partials. As discussed in the previous section, H-dislocation interactions (attractive or repulsive) will arise if H occupies sites other than the local minimum binding energy sites. These interactions result in changing the relative position of the dislocation with respect to the H-array [24]. However, by introducing two H-arrays at opposite sides of the centerline of the dislocation, the SF width of both edge and screw dislocations can either increase or decrease depending on the occupying sites and positions of the two H-arrays relative to the minimum/maximum binding energy sites [24].

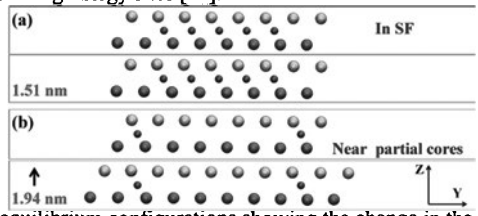

Figure 3. Initial and equilibrium configurations showing the change in the SF width of a screw: (a) H-arrays (purple spheres) in the SF; and (b) two H-arrays near the partial cores.

Figure 3a shows the effect of introducing a uniform distribution of H-arrays with line density 2 atoms/nm at T'-sites in the SF. Clearly, the SF width stays the same after relaxation. On the contrary, if H-arrays were only introduced near the partial cores, the SF width will increase to 1.94 nm, as shown in Fig 3b. This is in agreement with the saturated width computed by Wen *et al* for the uniform distribution of H on the dislocation glide plane [15, 16]. These results are consistent with the binding energy calculations discussed in the previous section that the occupation sites in the SF (|Y| < 4.5 angstrom) have binding energies close to the minimum energy; as a result, the H-dislocation interaction is very weak. Thus, only H-atoms occupying T'-sites near the Shockley partial cores (|Y| > 4.5 angstrom) can increase the SF width.

In view of these current results, the observed increase in the SF width as a function of uniform H-concentration on the glide plane (i.e. areal H-concentration) reported by Wen *et al* [15,16] can be explained. For low areal H-concentrations, the probability of H-atoms occupying sites very close to the Shockley partials is small and thus the change in the SF width is minimal. On the other hand, by increasing the areal H-concentration this probability increases, and thus the SF width will increase. As reported by Wen *et al.* [15] a saturation limit in the SF width is reached at some areal concentrations, which can be explained here as the necessary 'uniform' areal density required for H to occupy T'-sites near the Shockley partials of the dislocation. As clear from our study, the H-concentration is not really the driving phenomenon in controlling the SF width, but rather the occupying site and their relative position to the minimum binding sites.

Hydrogen Effects on the Generalized Stacking Fault Energy

In the presence of interstitial H, it has been hypothesized [15] that the SF width in FCC Ni should increase due to the decrease in the stable SFE [27]. The GSFE profile for FCC Ni sheared in the $[11\bar{2}]$ direction along the (111) plane is shown in Figure 4a. This energy profile defines several important features of slip, including the stable (or intrinsic) SFE, $\gamma_{sf} = 87.8$ mJ/m^2, and the unstable SFE, $\gamma_{us} = 212$ mJ/m^2. In the presence of H, the GSFE as a function of H-concentration in the SF plane is shown in Figure 4b. The GSFE with an H areal density of 1.16 atoms/nm^2 is shown as red dash-dot-dot line in Figure 4b. The unstable SFE clearly increased to $\gamma^H_{us} = 224$ mJ/m^2, indicating an impeding effect during shear, while the stable SFE decreased to $\gamma^H_{sf} = 72.5$ mJ/m^2. In addition, a discontinuity in the GSFE curve is observed due to H-atoms jumping from O-sites to their nearest T'-sites. To avoid this discontinuity, H-atoms were forced to move proportionally from the initial O-sites to the nearest T'-sites as the upper half moves from FCC sites to HCP sites. In this case the GSFE (red circle-line in Figure 4b) deviates slightly from the case that H-atoms are allowed to move freely before the discontinuity, but overlaps with it after the jump. The unstable SFE here is $\gamma^H_{us} = 229$ mJ/m^2, and the stable SFE is $\gamma^H_{sf} = 72.5$ mJ/m^2, which is in very good agreement with the case where H moves freely. The GSFE for H-concentration of 3.48 atoms/nm^2 and 4.64 atoms/nm^2 show a similar behavior with unstable SFE increasing, and the stable SFE decreasing with increasing H-concentration.

The decrease in the stable SFE with increasing H-concentration arises from the negative binding energy of H occupying T'-sites in the SF. For the case of H-concentration of 1.16 atoms/nm^2, the binding energy is calculated to be $E_b = -0.0817$ eV/atom, which gives $E_b/A = -15.3$ mJ/m^2, where A is the area of the SF [24]. This accounts for the decrease in the stable SFE from 87.8 to 72.5 mJ/m^2. However, the decrease in the stable SFE does not necessitate an increase in the SF width. As shown by Kibey *et al* [28] using generalized P-N model, the SF width does not solely depend on the stable SFE, but also depends on the unstable and maximum SFE. As seen in Figure 4b, H in the SF region decreases the stable SFE, but also increases the unstable SFE. These two competing effects may cancel each other and lead to an unvarying SF

width, as observed in Figure 3a. On the other hand, if all H atoms were allowed to move in the direction perpendicular to the (111) plane and constrained from in plane motion, then the initial O-sites in FCC lattice will become O'-sites in SF after shearing. As a result, the stable SFE will increase significantly as shown in Figure 4b (green dashed line). This increase is due to the positive binding energy of O'-sites in the SF, and explains the increase in γ_{sf} with increasing H-concentration reported by von Pezold *et al* [17]. However, O'-sites are not preferential occupying sites for H in the SF, and H atoms will diffuse to the nearest T'-site during shear.

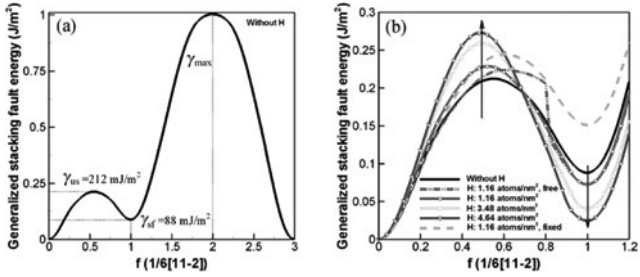

Figure 4. Generalized stacking fault energy of $[1\bar{1}2](111)$ slip system (a) without and (b) with H.

Hydrogen Effects on Dislocation-intersection Induced Cross-slip

An athermal cross-slip mechanism of screw dislocation induced by dislocation-intersection has been recently observed through atomistic simulations by Rao *et al* [26]. The H-free relaxed configuration is shown in Figure 5b with an instantaneous cross-slipped segment forming on the (1-11) at the intersection with a forest dislocation (line direction [0-1-1], b =1/2[10-1] in (1-11) plane). For this specific interaction no activation energy for cross-slip is required. It should be noted that under certain conditions cross-slip is athermal and spontaneous with zero activation energy while in other intersection configurations a finite thermal activation energy exists. Full details of these different configurations can be found in our previously published work [26, 29].

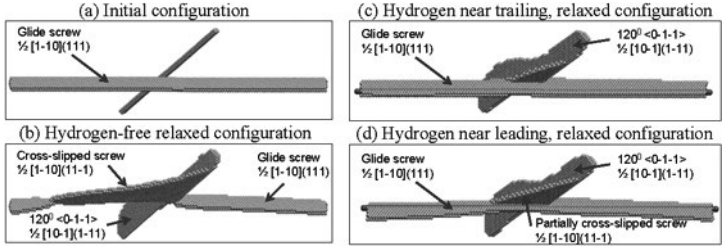

Figure 5. (a) Initial and (b) relaxed configurations showing instantaneous cross-slip; (c) and (d) relaxed configurations showing cross-slip with H-array occupying different positions.

In the presence of an H-array with line density of 4 atoms/nm occupying T'-sites in the SF of the screw, the dislocation-intersection induced cross-slip was inhibited by pinning of the trailing partial, as shown in Figures 5c and 5d. When the H-array was introduced in the SF close to the trailing partial, the leading partial still can react with one of the forest partial, forming a stair-rod dislocation. However, the screw dislocation is not able to fold onto the cross-slip plane, since the trailing partial is pinned. When the H-array was introduced in the SF close to the

leading partial, the trailing is able to move toward the leading partial due to the screw-forest interaction until it hits the H-array and gets pinned. With H-array line density as low as 1 atom/nm, the cross-slip is still partially inhibited. The pinning of dislocation by H in the SF is consistent with the fact that the unstable SFE is increased in the presence of H and the lattice resistance to shear is increased.

Conclusion

In this comprehensive study it was shown that the strongest H-binding sites to an edge dislocation are octahedral-sites in the tension region near the partial dislocation core on one plane above the dislocation glide plane (tension region). For screw dislocations, both tetrahedral-sites in the SF and octahedral-sites near one of the two Shockley partial cores on one plane above/below have the strongest binding energy. An attractive or a repulsive interaction between hydrogen and the screw or edge dislocations depends on the relative position of the hydrogen to these strongest binding sites. The SF width may increase or decrease, also depending on the H-occupying sites and the relative position of the hydrogen to the strongest binding sites. The stable SFE decreases with increasing hydrogen concentration due to the resulting negative binding energy to the SF. On the other hand, the unstable SFE increases with increasing H concentration, which may result in pinning the dislocation. These fundamental understandings provide a clearer physical basis of the interactions between interstitial hydrogen and defects (stacking faults and dislocations) in FCC metals, and may aid in providing a better physical interpretation of the two main hypothesized mechanisms governing hydrogen embitterment, namely hydrogen enhanced localized plasticity (HELP) [30,31]and hydrogen enhanced decohesion (HEDE) [32].

References

1. A. Pundt and R. Kirchheim, "Hydrogen in Metals: Microstructureal aspects," *Annu. Rev. Mater. Res.*, 36 (2006), 555-608.
2. I.M. Robertson, "The Effect of Hydrogen on Dislocation Dynamics," *Eng. Fract. Mech.*, 68 (2001), 671-692.
3. A. Barnoush and H. Vehoff, "Recent Developments in the Study of Hydrogen Embrittlement: Hydrogen Effect on Dislocation Nucleation," *Acta Mater.*, 58 (2010), 5274-5285.
4. H.K. Birnbaum and P. Sofronis, "Hydrogen-enhanced Localized Plasticity Mechanism for Hydrogen-related Fracture," *Mater. Sci. Eng. A*, 176 (1994), 191-202.
5. S. Asano and R. Otsuka, "The Lattice Hardening due to Dissolved Hydrogen in Iron and Steel," *Scripta Metall.*, 10 (1976), 1015-1020.
6. A. Kimura and H.K. Birnbaum, "Plastic Softening by Hydrogen Plasma Charging in Pure Iron," *Scripta Metall.*, 21 (1987), 53-57.
7. Y. Yagodzinskyy and H. Hanninen, "Hydrogen-dislocation Interactions and Their Role in HELP Mechanism of Hydrogen Embrittlement," *Proc. 11th Inter. Conf. Fract.* (Turin, Italy, 2005).
8. D. Abraham and C. Altstetter, "The Effect of Hydrogen on the Yield and Flow Stress of an Austenitic Stainless Steel," *Metall. Mater Trans. A*, 26 (1995), 2849-2858.
9. T.J. Marrow, C.A. Hippsley, and J. E. King, "Effect of Mean Stress on Hydrogen Assisted Fatigue Crack Propagation in Duplex Stainless Steel," *Acta Metall. Mater.*, 39 (1991), 1367-1376.
10. C. Skipper et al., "Effect of Internal Hydrogen on Fatigue Strength of Type 316 Stainless Steel," *Proc. 2008 Inter. Hydrogen Conf.*, ed. B. Somerday, P. Sofronis, and R. Jones (AMS International, Materials Park, Ohio, USA, 2009), 139-146.

11 . Y. Murakami, T. Kanezaki, and Y. Mine, "Hydrogen Effect against Hydrogen Embrittlement," *Metall. Mater. Trans. A*, 41 (2010), 2548-2562.
12. M.S. Daw et al., "Application of the Embedded Atom Method to Fracture, Dislocation Dynamics, and Hydrogen Embrittlement" (Sandia Report 86-8660, 1986).
13. S. Taketomi, R. Matsumoto, and N. Miyazaki, "Atomistic Simulation of the Effects of Hydrogen on the Mobility of Edge Dislocation in Alpha Iron," *J. Mater. Sci.*, 43 (2008), 1166-1169.
14. J. Song and W.A. Curtin, "A Nanoscale Mechanism of Hydrogen Embrittlement in Metals," *Acta Mater.*, 59 (2011), 1557-1569.
15. M. Wen, S. Fukuyama, and K. Yokogawa, "Atomistic Simulations of Hydrogen Effect on Dissociation of Screw Dislocations in Nickel," *Scripta Mater.*, 52 (2005), 959-962.
16. M. Wen, S. Fukuyama, and K. Yokogawa, "Cross-slip Process in fcc Nickel with Hydrogen in a Stacking Fault: An Atomistic Study using the Embedded-atom Method," *Phys. Rev. B*, 75 (2007), 144110.
17. J. von Pezold, L. Lymperakis, and J. Neugebeauer, "Hydrogen-enhanced Local Plasticity at Dilute Bulk H Concentrations: The Role of H-H Interactions and the Formation of Local Hydrides," *Acta Mater.*, 59 (2011), 2969-2980.
18. S. Plimpton, "Fast Parallel Algorithms for Short-Range Molecular Dynamics," *J. Comp. Phys.*, 117 (1995), 1-19.
19. J. Angelo, N.R. Moody, and M.I. Baskes, "Trapping of Hydrogen to Lattice Defects in Nickel," *Modell. Simul. Mater. Sci. Eng.*, 3 (1995), 289-307.
20. M.I. Baskes et al., "Trapping of Hydrogen to Lattice Defects in Nickel," *Modell. Simul. Mater. Sci. Eng.*, 5 (1997), 651-652.
21. H. Tsuzuki, P.S. Branicio, and J.P. Rino, "Structural Characterization of Deformed Crystals by Analysis of Common Atomic Neighborhood," *Comput. Phys. Commun.*, 177 (2007), 518-523.
22. W. Humphrey, A. Dalke, and K. Schulten, "VMD - Visual Molecular Dynamics," *J. Molec. Graphics*, 14 (1996), 33-38.
23. A.N. Stroh, "Dislocations and Cracks in Anisotropic Elasticity," *Phil. Mag.*, 3 (1958), 625-646.
24. Y. Tang and J.A. El-Awady, "Atomistic Simulations of the Interactions of Hydrogen with Dislocations in fcc Metals," *Phys. Rev. B*, (2012), 004100 (in press).
25. V. Vitek, "Intrinsic Stacking Faults in Body-centred Cubic Crystals," *Phil. Mag.*, 18 (1968), 773-786.
26. S.I. Rao, et al., "Investigation of Spontaneous Athermal Cross-Slip Nucleation at Screw Dislocation Intersections in FCC Metals and $L1_2$ Intermetallics Using Atomistic Simulations," *Acta Mater.*, submited, 2012.
27. R.H. Windle and G.C. Smith, "The Effect of Hydrogen on the Plastic Deformation of Nickel Single Crystals," *Mater Sci. J.*, 2 (1968), 187-191.
28. S. Kibey et al., "Effect of Nitrogen on Generalized Stacking Fault Energy and Stacking Fault Widths in High Nitrogen Steels," *Acta Mater.*, 54 (2006), 2991-3001.
29. S.I. Rao, et al., "Activated states for cross-slip at screw dislocation intersections in face-centered cubic nickel and copper via atomistic simulation," *Acta Mater.*, 58 (2010), 5547-5557.
30. C.D. Beachem, "A New Model for Hydrogen-assisted Cracking (Hydrogen Embrittlement)," *Metall. Mater. Trans. B*, 3 (1972), 441-455.
31. S.P. Lynch, "Environmentally Assisted Cracking: Overview of Evidence for an Adsorption Induced Localised-slip Process," *Acta Metall.*, 36 (1988), 2639-2661.
32. C.A. Zapffe and C. E. Sims, "Hydrogen Embrittlement, Internal stress, and Defects in Steel," *Trans. AIME*, 145 (1941), 225-259.